RSC Advances

PAPER

View Article Online
View Journal | View Issue

Cite this: *RSC Adv.*, 2017, **7**, 34687

Simultaneous reductive and sorptive removal of Cr(VI) by activated carbon supported β-FeOOH†

Tingting Yang,[a] Lirong Meng,[a] Shuwen Han,[a] Jianhua Hou,[ab] Shengsen Wang[ab] and Xiaozhi Wang *[ab]

An activated carbon (AC)-supported nanocomposite was prepared by precipitating β-FeOOH onto KOH activated soybean meal-derived biochar (SYBK). The as-prepared β-FeOOH/SYBK composites were characterized by N_2-Brunauer–Emmett–Teller (BET), scanning electron microscopy (SEM), X-ray diffractions (XRD) and X-ray photoelectron spectroscopy (XPS). XRD results confirmed that β-FeOOH was impregnated by AC. The chromate (Cr(VI)) removal capacity was investigated in a batch experiment with different conditions. The ratios of β-FeOOH and AC were compared for Cr(VI) removal and a loading quantity of 20 wt% β-FeOOH was considered as the most efficient amount. This was possibly ascribed to it having the highest surface area (670.65 $m^2\ g^{-1}$) of the β-FeOOH/SYBK nanocomposites. It was found that 20β-FeOOH/SYBK could remove as much as 96% Cr(VI) at pH 1–2 with 2 mmol L^{-1} EDTA and 2.0 g L^{-1} nanocomposites. The maximal Cr(VI) removal by 20β-FeOOH/SYBK was 37.04 g kg^{-1}, as estimated by a Langmuir isotherm model. The removal mechanisms were examined by studying the speciation of Cr on sorbents as well as in aqueous solution. The XPS analysis of spent sorbents and chemical speciation of Cr in aqueous solutions revealed that partial Cr(VI) was reduced to Cr(III) on sorbents and in aqueous solution. This suggests that Cr(VI) can be removed by simultaneous sorption and reduction by the as-prepared nanocomposites.

Received 8th June 2017
Accepted 3rd July 2017

DOI: 10.1039/c7ra06440c

rsc.li/rsc-advances

1. Introduction

Chromium (Cr) is a typical toxic heavy metal, which has been extensively used in electroplating, leather tanning and other industrial applications.[1,2] Excessive accumulation in the human body may cause serious health problem.[3] The U.S. Environmental Protection Agency has prescribed a maximal allowance concentration of 0.1 mg L^{-1} in drinking water.[4] Cr exists mainly in two stable valence states, namely hexavalent Cr (Cr(VI)) and trivalent Cr (Cr(III)), with different toxicity, mobility and biological availability. In contrast to Cr(III), Cr(VI) exists as CrO_4^{2-} and $Cr_2O_7^{2-}$ in the solution, which is more toxic and soluble. The toxicity of Cr(VI) is 100 times higher than Cr(III).[5] To reduce Cr(VI) toxicity in contaminated soil and water, Cr(VI) can be removed by sorption or reduced to its less toxic form.[6,7]

Activated carbon (AC) is a carbon-enriched material, which is characterized with high surface area and abundant functional groups.[8] The favorable properties enable it to remove many kinds of organic and inorganic contaminants from aqueous solutions. Recently, the reduction of Cr(VI) in water treatment has been achieved by various biochar,[9] *e.g.*, derived from agricultural and forestry waste. In this study, soybean meal was used to produce biochar (BC) with abundant elements such as Si, Mg, Al, and so on. Chemical activation may increase the surface area and functional groups of biochars. KOH activation was an effective method to prepare AC and to increase its surface area,[10,11] and activated carbon can be widely used as an sorbent in waste water treatment.[12,13] However, most carbonaceous materials such as activated carbon are not efficient for Cr(VI) removal,[14,15] which is possibly ascribed to the low point zero charges and negative zeta potential at neutral pH. The negative charges at normal environmental conditions of the sorbents is not favorable for sorption of negatively charged Cr(VI).[16] As a result, various materials are incorporated in the carbon matrix to improve its performance for Cr(VI) removal.

Iron oxide is an ideal candidate which can not only adsorb Cr(VI) but also reduce it to a less toxic species.[17] Akaganéite (β-FeOOH) is a typical iron oxyhydroxide mineral and characterized with a channel structure parallel to the *c*-axis.[18] β-FeOOH is widely used as sorbents as well as a Fenton-like catalyst to remove contaminants from aqueous solutions.[19] Both sorptive and reductive removal of Cr(VI) by β-FeOOH has been reported elsewhere.[20] The Fe(III) can then be transformed to Fe(II),[21] largely dependent onto conditions of the reactions. β-FeOOH is usually synthesized by wet-chemistry approach, and the prepared nanoparticles may aggregate which is difficult to

[a]*College of Environmental Science and Engineering, Yangzhou University, Jiangsu 225127, China. E-mail: xzwang@yzu.edu.cn*

[b]*Jiangsu Collaborative Innovation Center for Solid Organic Waste Resource Utilization, Nanjing 210095, China*

† Electronic supplementary information (ESI) available. See DOI: 10.1039/c7ra06440c

separate from aqueous solutions. Activated carbon is a commonly-used support matrix to stabilize nanoparticles. Thus, we propose to immobilize β-FeOOH with activated carbon to improve its surface area and thus Cr(VI) removal capacity.

In this work, the KOH-activated carbons were impregnated with β-FeOOH. The purposes of this study were to (1) prepare and characterize the KOH activated soybean meal derived biochar, (2) select the most efficient β-FeOOH loadings onto activated carbon for Cr(VI) removal, (3) investigate the sorptive and reductive removal capacity of Cr(VI), and (4) find out the possible mechanisms associated with Cr(VI) removal.

2. Materials and methods

2.1 Chemical reagents

Cr(VI) aqueous solution was prepared by using potassium dichromate ($K_2Cr_2O_7$) of analytical grade. Potassium hydroxide (KOH), ethylene diamine tetra acetic acid (EDTA), ferric chloride hexahydrate ($FeCl_3 \cdot 6H_2O$), urea (H_2NCONH_2), potassium permanganate ($KMnO_4$) used were of analytical grade. 1 M HCl and NaOH were used to adjust the pH of Cr(VI) solution. Deionized (DI) water was used to dissolve the chemicals.

2.2 Modified biocahr preparation

To prepare soybean meal derived biochars (SYB), a commercial soybean meal was oven dried at 80 °C, and then pyrolyzed in a tube furnace at 700 °C for two hours purged with nitrogen gas. The BC was washed with DI water and oven dried overnight at 80 °C. The obtained SYB was mixed with KOH solution, with KOH : BC mass ratio of 1 : 1. The suspension was stirred for two hours and then heated at 80 °C until the mixture turned into a paste. The resulting product was heated (10 °C min^{-1}) in a tube furnace at a highest temperature of 800 °C for 1 h in N_2 flow. After cooling, the sample was washed with a 0.1 N HCl acid and DI water, oven dried overnight at 80 °C. The resulting activated carbon was denoted as SYBK.

Four β-FeOOH/SYBK composites, with the different loading percentage of β-FeOOH, were obtained by following procedures according to the previous method.[3] 0.5 g SYBK was added to 60 mL deionized water and magnetically stirred for 24 h. Then, the required amount of $FeCl_3 \cdot 6H_2O$ and urea (with β-FeOOH : SYBK mass ratio of 5 : 95, 10 : 90, 20 : 80, 40 : 60, and Fe^{3+}/urea mole ratio of 1 : 4) were added to the above suspension, respectively. After stirring for 60 min, the obtained slurry was transferred into a Teflon-lined stainless steel autoclave (100 mL) and was maintained at 90 °C for 8 h. The resulting composites were cooled to room temperature and filtered by suction filtration. The composites were then washed several times with ethanol and DI water, and oven dried overnight at 80 °C. The obtained samples were denoted as 5β-FeOOH/SYBK, 10β-FeOOH/SYBK, 20β-FeOOH/SYBK, 40β-FeOOH/SYBK, respectively. For comparison, β-FeOOH/SYB was prepared by SYB (without activated by KOH) following same procedure but with no KOH activation (with β-FeOOH : SYB mass ratio of 20 : 80, and the Fe^{3+}/urea mole ratio 1 : 4).

2.3 Characterization and analysis β-FeOOH/SYBK

The structure and phase of as-prepared β-FeOOH/SYBK samples were determined using an X-ray diffractometer (XRD, D8-ADVANCE) and X-ray electron spectroscopy (XPS, ESCALAB 250Xi). The surface morphology of β-FeOOH/SYBK was examined by scanning electron microscope (SEM, S-4800II). Nitrogen adsorption–desorption isotherms and specific surface areas were measured on a Micromeritics ASAP 2460, and surface area and pore volume was calculated with Brunauer–Emmett–Teller (BET) theory.

2.4 Cr(VI) removal experiments

The sorption of Cr(VI) by nanocomposites was carried out in a batch experiment. First, the optimal β-FeOOH loading was determined by adding different sorbents to 50 mg L^{-1} Cr(VI) solution, with pH adjusted at 2 and in presence of 2 mM EDTA. The Cr(VI) removal efficiency was examined as a function of time. A reaction time of 60 min was selected for subsequent experiments. Second, the most appropriate sorbent dosage was compared by adding different amounts of sorbents (0, 0.5, 1.0, 1.5, 2.0, and 2.5 g L^{-1}) to 50 mg L^{-1} Cr(VI) solution, with pH adjusted at 2 and in presence of 2 mM EDTA. Third, the sorption of Cr(VI) (50 mg L^{-1}) by 20β-FeOOH/SYBK at different pH was determined at pH of 1, 2, 3, 4 and 7, with EDTA of 2 mM. Then, the sorption isotherm by 20β-FeOOH/SYBK was conducted at pH of 2, with different Cr(VI) concentrations (10, 15, 25, 40, 50, 60 and 80 mg L^{-1}). The reactions were initiated in 50 mL vessels, and the suspension was shaken on a rotary shaker at 25 °C.

After reaction, the solutions were sampled at different time and then filtered through 0.45 μm membranes. Total Cr(VI) was analyzed with the 1,5-diphenylcarbazide colorimetric method (with potassium permanganate).[22] The concentrations of Cr(VI) was measured using the 1,5-diphenylcarbazide colorimetric method[23,24] with an UV/Vis spectrophotometer at 540 nm. The Cr(III) in solutions was analyzed by the difference of total Cr and Cr(VI).[25] The spent sorbents were analyzed with XPS to obtain the Cr speciation after sorption. The Fe(III) and Fe(II) in solutions was analyzed with 1,10-phenanthroline.[26]

3. Results and discussion

3.1 Characteristics of as-synthesized β-FeOOH/SYBK

Fig. 1 showed the XRD patterns of different BC, AC and β-FeOOH nanocomposites. The diffraction peaks of SYB at $2\theta^\circ$ = 26.62, 28.62, 42.92 could be indexed to (011) and (211) planes of quartz and (200) plane of periclase. After KOH activation, (200) and (220) planes of SYBK were observed, corresponding to periclase. After β-FeOOH loading, the characteristic peaks at $2\theta^\circ$ = 35.25 was observed for 20β-FeOOH/SYB and 20β-FeOOH/SYBK, indicating formation of β-FeOOH.[20]

Nitrogen adsorption/desorption presents a type-IV isotherm (Fig. S1†) demonstrating typical mesoporous characteristics of nanoparticles. The average pore sizes of BC, AC and β-FeOOH nanocomposites ranged between 2.67 and 6.96 nm (Table 1). 20β-FeOOH/SYBK has a specific surface of 670.65 m^2 g^{-1}. Compared with SYB, the specific surface area of SYBK increased

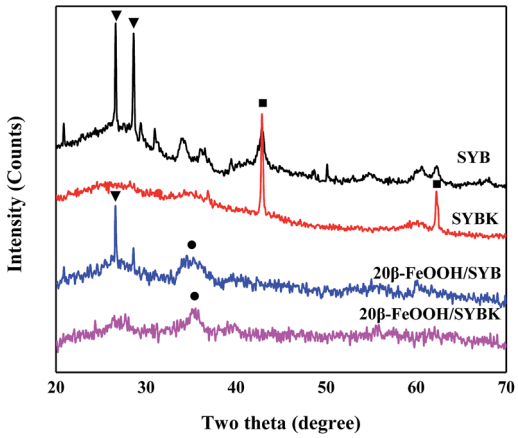

Fig. 1 XRD patterns of SYB, SYBK, 20β-FeOOH/SYB, 20β-FeOOH/SYBK.

Table 1 Surface area, average pore size and pore volume of BC, AC and β-FeOOH nanocomposites

Sample	S_{BET}[a] ($m^2\ g^{-1}$)	Average pore size[b] (nm)	Pore volume[c] ($cm^3\ g^{-1}$)
SYB	14.76	6.955	0.026
SYBK	477.71	2.713	0.324
20β-FeOOH/SYB	171.24	3.835	0.164
20β-FeOOH/SYBK	670.65	2.666	0.447

[a] Note: surface area was calculated with Brunauer–Emmett–Teller (BET) method. [b] Estimated from the Barrett–Joyner–Halenda (BJH) formula. [c] Single point adsorption total pore volume of pores.

nearly by 32 times from 14.76 $m^2\ g^{-1}$ to 477.71 $m^2\ g^{-1}$, and the pore volume also increased about 12 times from 0.026 $cm^3\ g^{-1}$ to 0.324 $cm^3\ g^{-1}$. This is possibly attributed to the surface reaction occurred on the interface of BC and KOH during the activation, which promote pore formation.[27] β-FeOOH impregnation also increased the specific area of SYB and SYBK, possibly because the blocked pores are liberated or new pores were crated during β-FeOOH loading.[28]

SEM images showed that SYB exhibited carbon skeletons (Fig. S2a†). After KOH activation, the surface of SYBK (Fig. S2b†) became more porous, and the most pores were maintained even after β-FeOOH loading (Fig. S2d†).

The XPS spectra of 20β-FeOOH/SYBK showed a considerable amount of Fe appeared in composites (Fig. 2). The C 1s spectra showed peaks at binding energies (BEs) of 287.3 eV, 285.98 eV and 289.48 eV, corresponding to C–O, hydroxyl (C–OH) bond,[29] carbonyl (O–C=O) bond,[30] respectively. The O 1s spectra (Fig. 2c) show the positions of Fe–O–H bonds with BE of 531.06 eV, Fe–O–C bonds at 532.2 eV,[31,32] organic C=O bonds at 533.38 eV. The peak with BE of 534.38 eV indicated the formation of C–O. The presence of Fe–O and Fe–O–H bonds suggest the formation of β-FeOOH.[33] BE peaks of Fe 2p spectrum with 712.2, 718.9, 726.3 and 733.6 eV corresponded to Fe(III).[34]

3.2 Cr(VI) removal from aqueous solutions

3.2.1 Effects of β-FeOOH loading on Cr(VI) removal kinetics. The Cr(VI) removal kinetics by β-FeOOH nanocomposites was described by pseudo-first-order kinetics (Fig. 3B). The rate constant, k, was summarized in Table 2. Rate constants of SYB and SYBK were several times lower than

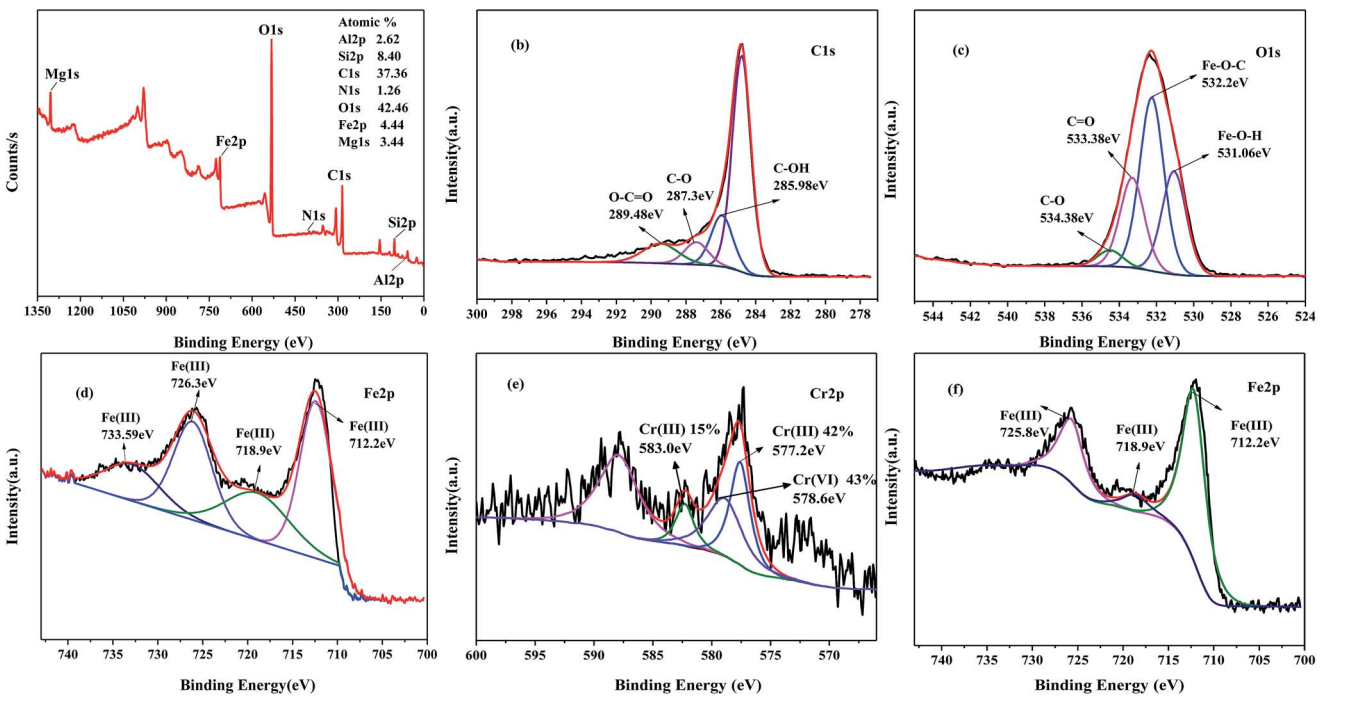

Fig. 2 (a) XPS spectra of 20β-FeOOH/SYBK before, high-resolution XPS spectra of (b) C 1s, (c) O 1s, (d) Fe 2p and after Cr(VI) reduction Cr 2p (e), Fe 2p (f).

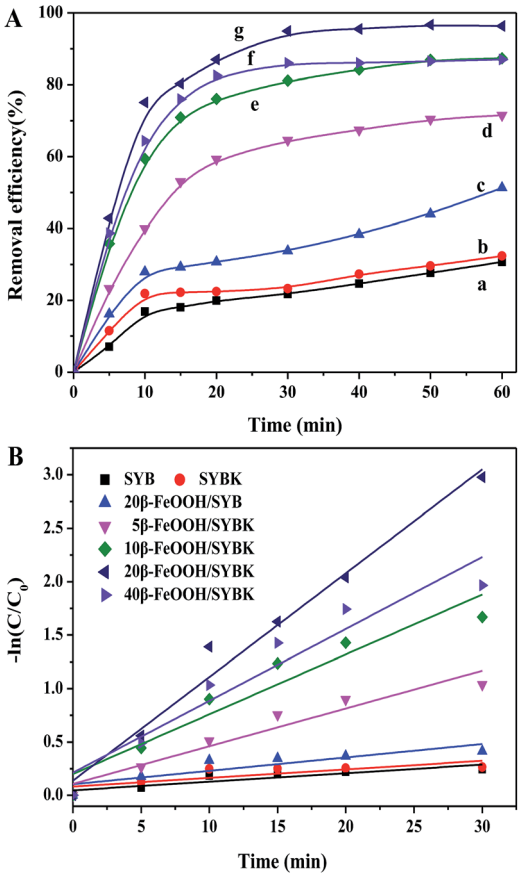

Fig. 3 The removal efficiency of Cr(VI) in different system with reaction time. (A) (a) SYB; (b) SYBK; (c) 20β-FeOOH/SYB; (d) 5β-FeOOH/SYBK; (e) 10β-FeOOH/SYBK; (f) 40β-FeOOH/SYBK; (g) 20β-FeOOH/SYBK. Reaction conditions: 2g L^{-1} synthesis, 2 mM EDTA, 49.21 mg L^{-1} Cr(VI), pH = 2.0. (B) Pseudo-first-order kinetic corresponding to (A).

Table 2 Pseudo-first-order kinetics for Cr(VI) removal by sorbents

Synthesis	Kinetic constant, k (10^{-2} min^{-1})	Coefficient of determination, R^2
SYB	0.801	0.762
SYBK	0.802	0.569
20β-FeOOH/SYB	1.255	0.706
5β-FeOOH/SYBK	3.536	0.916
10β-FeOOH/SYBK	5.602	0.901
20β-FeOOH/SYBK	9.710	0.975
40β-FeOOH/SYBK	6.728	0.905

activated carbon impregnated with β-FeOOH. That is, β-FeOOH impregnation greatly increased rate constant of Cr(VI) removal, where β-FeOOH accounted for about 12 times greater reaction rates as compared to pristine biochar.

Cr(VI) removal efficiency was 30.7% and 32.4% for SYB and SYBK within 60 min. β-FeOOH greatly increased Cr(VI) removal efficiency. The Cr(VI) removal decreased in the following order: 20β-FeOOH/SYBK > 10β-FeOOH/SYBK > 40β-FeOOH/SYBK > 5β-FeOOH/SYBK. β-FeOOH/SYBK was more capable of Cr(VI) removal than β-FeOOH/SYB (Fig. 3A).

3.2.2 Effect of EDTA concentrations. EDTA can chelate with HMs and significantly enhance the reaction rate and removal efficiency of Cr(VI).[35] As shown in Fig. 4, the effect of coexisting EDTA concentration (0 to 4.0 mmol L^{-1}) on the removal efficiency of Cr(VI) was investigated at pH of 2 with 2.0 g L^{-1} 20β-FeOOH/SYBK. The Cr(VI) removal generally increased with EDTA concentration up to 2.0 mmol L^{-1}, which amount to 96% Cr removal. EDTA is expected to chelate with Cr and Fe in solution, which prevents its precipitation and thus increase contact between two cations. However, 4.0 mmol L^{-1} EDTA decreased Cr(VI) removal, implying overdosage of EDTA may compete with Cr(VI) for the adsorption sites on the as-prepared β-FeOOH nanoparticles surface.

3.2.3 Effect of sorbent dosage on Cr(VI) removal. The effect of sorbent dosage (0 to 2.5 g L^{-1}) on the removal efficiency of Cr(VI) was investigated at pH 2 in the presence of 2 mM EDTA. As shown in Fig. 5, the Cr(VI) removal efficiency was 19% with 2 mM EDTA only. By contrast, the Cr(VI) removal increased rapidly with the dosage up to 2.0 g L^{-1}, which amount to 96% Cr(VI) removal. A minor 2% increase occurred when dosage was increased from 2.0 g L^{-1} to 2.5 g L^{-1}, and thus 2.0 g L^{-1} was selected in subsequent experiment.

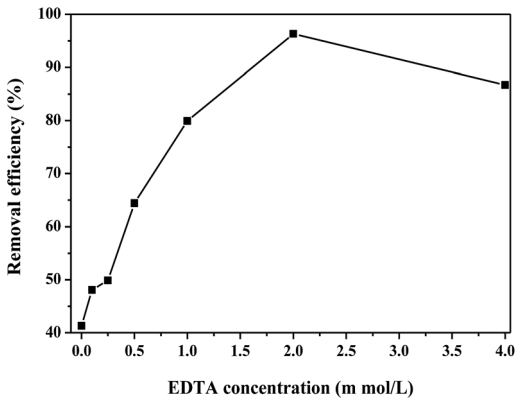

Fig. 4 Effects of EDTA concentration on Cr(VI) reduction efficiency (cCr(VI) = 50 mg L^{-1}; pH = 2; synthesis (20β-FeOOH/SYBK) dosage = 2g L^{-1}).

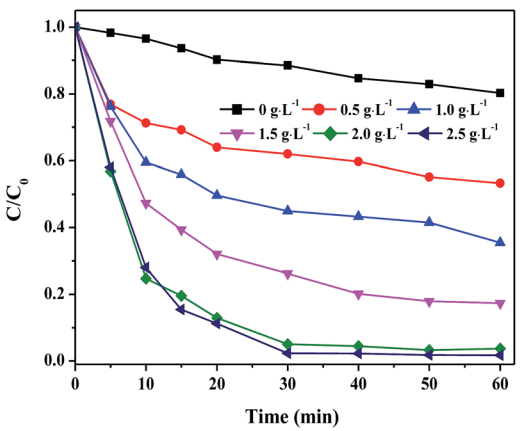

Fig. 5 Effects of synthesis (20β-FeOOH/SYBK) dosage on Cr(VI) reduction efficiency (cCr(VI) = 50 mg L^{-1}; pH = 2; c(EDTA) = 2 mM).

3.2.4 Effect of pH on Cr(VI) removal. Since the redox potentials of Cr(VI) species (H_2CrO_4, $HCrO_4^-$, CrO_4^{2-} and $Cr_2O_7^{2-}$) greatly depend on the solution pH,[36] the effects of pH on Cr(VI) removal was also investigated. The Cr(VI) removal efficiency increased as the solution pH dropped (Fig. 6). About 96% and 99% Cr(VI) was removed at pH 1 and 2, while only 8% Cr(VI) was removed at pH 7 after 60 min. The lower Cr(VI) removal at pH 4 or above is possibly associated with declined adsorption and thermodynamic driving force.[37] Besides, precipitation of Cr(VI) or Cr(III) may block the reactive sites at high pH value, which reduced Cr(VI) removal.[38,39]

3.2.5 Adsorption isotherm. The Cr(VI) sorption isotherm data was simulated with Freundlich (eqn (1)) and Langmuir (eqn (2)) models (Fig. 7), the Cr(VI) sorption isotherm data was simulated with Freundlich (eqn (1)) and Langmuir (eqn (2)) models (Fig. 7).

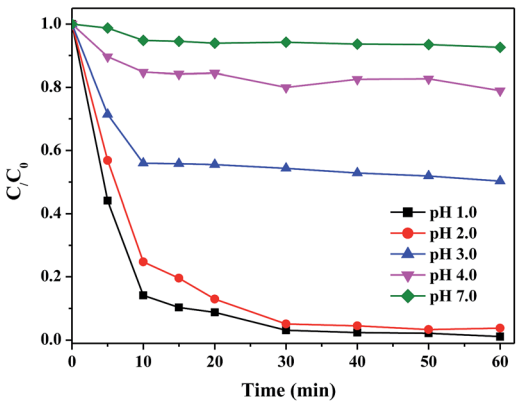

Fig. 6 Effects of initial suspension pH on Cr(VI) reduction efficiency (cCr(VI) = 50 mg L^{-1}; synthesis (20β-FeOOH/SYBK) dosage = 2g L^{-1}; c(EDTA) = 2 mM).

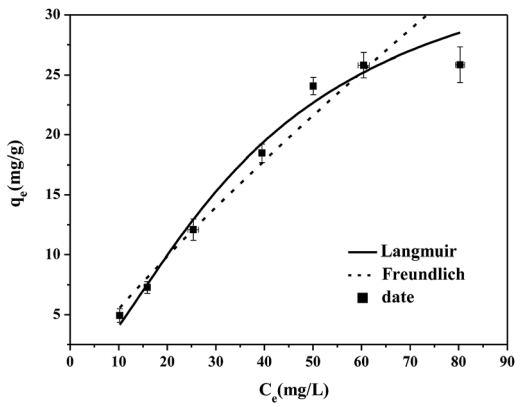

Fig. 7 Cr(VI) sorption isotherm data and fitted models for modified activated carbon (20β-FeOOH/SYBK).

$$\ln q_e = \ln K_f + 1/n \ln C_e \quad (1)$$

$$C_e/q_e = 1/(bq_m) + C_e/q_m \quad (2)$$

where q_e is the equilibrium adsorption capacity, mg g^{-1}; C_e is the equilibrium Cr(VI) concentration, mg L^{-1}; b (L mg^{-1}) and q_m (mg g^{-1}) are the Langmuir parameter and the maximum adsorption capacity, respectively; n and K_f represent the Freundlich constant and affinity coefficient.

Both models fitted the isotherm data well with R^2 above 0.91 (Table 3). The better fit was observed for Langmuir model with greater R^2. The maximal Cr(VI) removal by 20β-FeOOH/SYBK composite was estimated as 37.04 g kg^{-1} (Table 3). Thus, the adsorption of Cr(VI) to the 20β-FeOOH/SYBK mainly followed the Langmuir surface adsorption mechanisms. Comparison of Cr(VI) removal capacity with other work (Table 4) showed that the as-prepared β-FeOOH nanoparticles showed excellent Cr(VI) removal capacity than many other sorbents and was suggested as the best sorbent among carbon-based materials.

3.2.6 Proposed Cr(VI) removal mechanism. Excellent Cr(VI) removal was achieved by the β-FeOOH impregnated activated carbon. The elevated Cr(VI) removal was mainly ascribed to β-FeOOH as the active sites. It is expected that Cr(VI) removal would increase as more β-FeOOH was loaded, because sorption sites would increase as well. However, over-loading of β-FeOOH, *e.g.*, in 40FeOOH/SYBK, was not able to increase Cr(VI) removal evidently compared to 20β-FeOOH/SYBK. This was possibly due to the high aggregation of the nanoparticles which reduce its specific surface area. This was supported by low Cr(VI) removal of 20β-FeOOH/SYB which has low surface area, relative to 20β-FeOOH/SYBK.

In order to examine Cr(VI) removal mechanism by β-FeOOH, XPS was used to investigate the valence states of Cr and Fe on surface of 20β-FeOOH/SYBK after the reaction. The BE of Fe 2p at 725.8 eV, 718.9 eV and 712.4 eV can be interpreted as Fe(III) (Fig. 2f). The spectra of the Cr 2p have three BE peaks, namely Cr $2p_{3/2}$ (578.2 eV), Cr $2p_{1/2}$ (583.0 eV) and Cr $2p_{1/2}$ (587.7 eV) (Fig. 2e). The XPS-peak-differentiating analysis revealed Cr $2p_{3/2}$ could be divided into two peaks at BEs of 578.6 and 577.2 eV, corresponding to Cr(VI) and Cr(III), respectively. The peak at 783.0 eV is a characteristic peak of Cr(III). This suggests that both Cr(VI) and Cr(III) coexist on the surface of 20β-FeOOH/SYBK after reacting with 50 mg L^{-1} Cr(VI). The ratio of Cr(III)/Cr(VI) was found to be 1.4, indicating the sorption along with surface reduction was the dominant mechanisms. Besides, the concentration of total Cr decreased by 43% compared with

Table 3 Isotherms models and best fit parameters for Cr(VI) adsorption onto 20β-FeOOH/SYBK

	Langmuir			Freundlich		
Sample	q_m (g kg^{-1})	b (L mg^{-1})	R^2	K_f/(g kg^{-1})	1/n	R^2
20β-FeOOH/SYBK	37.036	0.0054	0.9799	0.764	0.8541	0.9483

Table 4 Comparison of the maximum Cr(VI) adsorption capacity of various adsorbents

Adsorbents	Sorbent dosage ($g\ L^{-1}$)	pH	Time	Cr sorption capacity ($g\ kg^{-1}$)	Reference
Biochar	4.0	2	24 h	24.6	40
Carbon slurry	4.0	2	70 min	15.24	41
Activated alumina	10	3	240 min	25.57	42
Activated carbon	4.0	3	180 min	3.46	14
Pomegranate husk carbon	3.0	1	180 min	35.2	43
Carbon nanotube	0.4	2	240 min	9.0	44
Fe_3O_4 nanoparticles	20	2	30 min	12.43	45
nZVI	1.0	2	250 min	148	46
α-Fe_2O_3	2.0	2	120 min	17.65	47
Crosslinked chitosan resins	2.0	3	120 min	84.19	48
Activated carbon supported β-FeOOH	2.0	2	60 min	37.04	Present work

Table 5 Effluent concentrations for Cr(VI) species after 60 min. (Reaction conditions: 2 $g\ L^{-1}$ synthesis, 2 mM EDTA, 50 $mg\ L^{-1}$ Cr(VI), pH = 2.0)

	Total Cr ($mg\ L^{-1}$)	Cr(VI) ($mg\ L^{-1}$)	Cr(III) ($mg\ L^{-1}$)
EDTA	49.73	40.15	9.58
20β-FeOOH/SYBK + EDTA	28.75	1.59	27.16

control treatment. Cr speciation was analyzed in the solution, which suggested that about 95% of Cr(VI) was reduced to Cr(III) after 60 min (Table 5). Thus, the Cr(VI) can be removed by sorption onto and reduction by the β-FeOOH.

According to high-resolution XPS spectra, Fe(III) was the ultimate species, but conversion of Fe(III) to Fe(II) was possibly happened in acidic condition during the process.[49] To further investigate the mechanisms associated with Cr(VI) removal by β-FeOOH nanocomposites, we measured content of total Fe, Fe(III) and Fe(II) concentrations in acidic solution (pH = 2) after 60 min reaction. The results showed Fe(II) percent was 20% (out of total dissolved Fe 6.88 $mg\ L^{-1}$) and 4% (out of total dissolved Fe 21.73 $mg\ L^{-1}$) in system with no and with Cr(VI). Lower Fe(II) with presence of Cr(VI) suggests partial Fe(II) can be oxidized by Cr(VI), which was evidenced by appearance of Cr(III) in XPS spectra. Consequently, the following reaction mechanisms were proposed in the low pH conditions. On one hand, Cr(VI) was sorbed by β-FeOOH nanocomposites. One other hand, the Fe(III) was partially converted to Fe(II) in very acidic condition (eqn (3)) on both surfaces of the sorbents and in bulk solutions. The Cr(VI) was then reduced by Fe(II) (eqn (4)), which was evidenced by identification of Cr(III) in both solutions and on surfaces of sorbents.

$$\beta\text{-FeOOH/activated carbon} \rightarrow Fe^{2+} + Fe^{3+} \quad (3)$$

$$3Fe^{2+} + CrO_4^{2-} + 4H_2O \rightarrow 3Fe^{3+} + Cr^{3+} + 8OH^- \quad (4)$$

4. Conclusions

The SYBK supported β-FeOOH nanocomposites were synthesized in a hydrothermal reaction with different β-FeOOH loading. The XRD analysis confirmed the successful synthesis of β-FeOOH on the activated carbon surfaces. The batch sorption experiment revealed that the efficient and economic β-FeOOH loading, pH and sorbent dosage were 20 wt%, 2, and 2 $g\ L^{-1}$, respectively. The predicted maximum Cr(VI) removal capacity was 37.04 $g\ kg^{-1}$ for 20β-FeOOH/SYBK composite. The enhanced removal efficiency of β-FeOOH/SYBK can be related to high surface area of sorbents. Both Cr(VI) and Cr(III) were identified in spent 20β-FeOOH/SYBK and solutions with XPS analysis. Thus, sorption and reduction were dominant Cr(VI) removal mechanisms by β-FeOOH/SYBK. The facile synthesis of sorbents and excellent Cr(VI) removal capacity indicated that as-prepared sorbents are good candidate for Cr(VI) remediation in aqueous solutions.

Acknowledgements

This work was supported in part by State Key Laboratory of Pollution Control and Resource Reuse (PCRRF1102), Social development project of Jiangsu Province (BE2015661), Six talent peaks project in Jiangsu Province (2013-NY-017). We thank the Testing Center of Yangzhou University for Sample Characterization.

References

1 A. Broadway, M. R. Cave, J. Wragg, F. M. Fordyce, R. J. F. Bewley, M. C. Graham, B. T. Ngwenya and J. G. Farmer, *Sci. Total Environ.*, 2010, **409**, 267–277.
2 C. Namasivayam and M. V. Sureshkumar, *Process Saf. Environ. Prot.*, 2007, **85**, 521–525.
3 Z. Xu, H. Jiang, Y. Yu, J. Xu, J. Liang, L. Zhou and F. Hu, *Appl. Clay Sci.*, 2017, **135**, 547–553.
4 Y. Xu and D. Zhao, *Water Res.*, 2007, **41**, 2101–2108.
5 P. L. Di, M. T. Gueye and E. Petrucci, *J. Hazard. Mater.*, 2015, **281**, 70–76.
6 T. Ölmez, *J. Hazard. Mater.*, 2009, **162**, 1371–1378.
7 K. P. Singh, A. K. Singh, S. Gupta and S. Sinha, *Desalination*, 2011, **270**, 275–284.
8 M. B. Ahmed, J. L. Zhou, H. H. Ngo and W. Guo, *Biomass Bioenergy*, 2016, **84**, 76–86.
9 Y. Han, X. Cao, X. Ouyang, S. P. Sohi and J. Chen, *Chemosphere*, 2016, **145**, 336–341.
10 Z. Hu and E. F. Vansant, *Carbon*, 1995, **33**, 1293–1300.
11 A. Ahmadpour and D. D. Do, *Carbon*, 1996, **34**, 471–479.
12 D. Mohan, K. P. Singh and V. K. Singh, *J. Hazard. Mater.*, 2008, **152**, 1045–1053.
13 X. Wang, N. Zhu and B. Yin, *J. Hazard. Mater.*, 2008, **153**, 22–27.
14 K. Selvi, S. Pattabhi and K. Kadirvelu, *Bioresour. Technol.*, 2001, **80**, 87.
15 I. Han, M. A. Schlautman and B. Batchelor, *Water Environ. Res.*, 2000, **72**, 29–39.
16 J. Wang, K. Zhang and L. Zhao, *Chem. Eng. J.*, 2014, **239**, 123–131.

17 I. B. Singh and D. R. Singh, *Environ. Technol.*, 2003, **24**, 1041.
18 Z. Y. Yuan, T. Z. Ren and B. L. Su, *Catal. Today*, 2004, **93**, 743–750.
19 Y. Zhao, H. Jiangyong and H. Chen, *J. Photochem. Photobiol., A*, 2010, **212**, 94–100.
20 M. Zhang, Z. Xu, J. Liang, L. Zhou and C. Zhang, *Int. J. Environ. Sci. Technol.*, 2015, **12**, 1669–1676.
21 Z. Xu, S. Bai, J. Liang, L. Zhou and Y. Lan, *Mater. Sci. Eng., C*, 2013, **33**, 2192.
22 S. C. Ponce, C. Prado, E. Pagano, F. E. Prado and M. Rosa, *Ecol. Eng.*, 2015, **74**, 33–41.
23 Q. Wang, X. Chen, K. Yu, Y. Zhang and Y. Cong, *J. Hazard. Mater.*, 2013, **246–247**, 135–144.
24 A. Idris, N. Hassan, N. S. Mohd Ismail, E. Misran, N. M. Yusof, A. F. Ngomsik and A. Bee, *Water Res.*, 2010, **44**, 1683–1688.
25 R. M. Cespón-Romero, M. C. Yebra-Biurrun and M. P. Bermejo-Barrera, *Anal. Chim. Acta*, 1996, **327**, 37–45.
26 A. E. Harvey Jr, J. A. Smart and E. S. Amis, *Anal. Chem.*, 1955, **27**, 26–29.
27 X. Yan, Q. Hu, X. Liu and Z. Yan, *Asia-Pac. J. Chem. Eng.*, 2012, **7**, 598–603.
28 A. Miura, K. Nakazawa, T. Takei, N. Kumada, N. Kinomura, R. Ohki and H. Koshiyama, *Ceram. Int.*, 2012, **38**, 4677–4684.
29 D. Yang, A. Velamakanni, G. Bozoklu, S. Park, M. Stoller, R. D. Piner, S. Stankovich, I. Jung, D. A. Field and C. A. Ventrice Jr, *Carbon*, 2009, **47**, 145–152.
30 A. Ganguly, S. Sharma, P. Papakonstantinou and J. Hamilton, *J. Phys. Chem. C*, 2011, **115**, 17009–17019.
31 A. N. Mansour and R. A. Brizzolara, *Surf. Sci. Spectra*, 1996, **4**, 357–362.
32 H. Abdel-Samad and P. R. Watson, *Appl. Surf. Sci.*, 1998, **136**, 46–54.
33 Y. Zheng, Z. Zhang and C. Li, *J. Mol. Catal. A: Chem.*, 2016, **423**, 463–471.
34 M. Ding, B. H. W. S. D. Jong, S. J. Roosendaal and A. Vredenberg, *Geochim. Cosmochim. Acta*, 2000, **64**, 1209–1219.
35 W. Qi, X. Shi, J. Xu, J. C. Crittenden, E. Liu, Z. Yi and Y. Cong, *J. Hazard. Mater.*, 2016, **307**, 213–220.
36 K. Kim and W. Choi, *Environ. Sci. Technol.*, 2011, **45**, 2202.
37 Y. Ku and I. L. Jung, *Water Res.*, 2001, **35**, 135–142.
38 T. Papadam, N. P. Xekoukoulotakis, I. Poulios and D. Mantzavinos, *J. Photochem. Photobiol., A*, 2007, **186**, 308–315.
39 W. D. Zhang, L. C. Jiang and J. S. Ye, *J. Phys. Chem. C*, 2009, **113**, 16247–16253.
40 A. Tytłak, P. Oleszczuk and R. Dobrowolski, *Environ. Sci. Pollut. Res.*, 2015, **22**, 5985–5994.
41 V. K. Gupta, A. Rastogi and A. Nayak, *J. Colloid Interface Sci.*, 2010, **342**, 135–141.
42 A. K. Bhattacharya, T. K. Naiya, S. N. Mandal and S. K. Das, *Chem. Eng. J.*, 2008, **137**, 529–541.
43 A. E. Nemr, *J. Hazard. Mater.*, 2009, **161**, 132–141.
44 M. A. Atieh, *Procedia Environ. Sci.*, 2011, **4**, 281–293.
45 S. H. Huang and D. H. Chen, *J. Hazard. Mater.*, 2009, **163**, 174–179.
46 H. Jabeen, V. Chandra, S. Jung, J. W. Lee, K. S. Kim and S. B. Kim, *Nanoscale*, 2011, **3**, 3583–3585.
47 Z. Jia, Q. Wang, D. Ren and R. Zhu, *Appl. Surf. Sci.*, 2013, **264**, 255–260.
48 Z. Wu, S. Li, J. Wan and Y. Wang, *J. Mol. Liq.*, 2012, **170**, 25–29.
49 S. S. Chen, C. Y. Cheng, C. W. Li, P. H. Chai and Y. M. Chang, *J. Hazard. Mater.*, 2007, **142**, 362.